J Mol Model (2005) 11: 17–25
DOI 10.1007/s00894-004-0213-x

ORIGINAL PAPER

Ugo Cosentino · M. Rosaria Varí
A. A. Gloria Saracino · Demetrio Pitea
Giorgio Moro · Mario Salmona

Tetracycline and its analogues as inhibitors of amyloid fibrils: searching for a geometrical pharmacophore by theoretical investigation of their conformational behavior in aqueous solution

Received: 22 July 2004 / Accepted: 1 September 2004 / Published online: 9 December 2004

Abstract Tetracycline (TC) and its derivatives have recently been proposed as a new class of antagonists in prion diseases as they prevent the aggregation of prion protein peptides and their acquisition of protease resistance in vitro and in vivo. Looking for relationships between conformational flexibility and biological activity, we searched for a geometrical pharmacophore by investigating, in aqueous solution, the conformational behavior of 15 TCs in both the zwitterionic and the anionic forms. For TC similar conformational flexibility was found for the two forms and two main conformational families were detected, an *extended* and a *folded* conformation characterized by different intramolecular hydrogen-bond networks. On comparing the Molecular Mechanics results with the ab initio ones and the experimental evidence, it can be seen that the conformational behavior of TC is reasonably well predicted by the MM2 force field, whereas the conformational energies provided by the Amber force field are unreliable. The conformational analysis of the other TC derivatives was then performed by the MM2 force field. As a result, their conformational behavior was similar to that observed for TC itself. Despite the hydronaphthacene moiety's conformational flexibility, no geometrical pharmacophore was found among the TCs, i.e. properties other than geometrical ones should play a crucial role in determining their anti-fibrillogenic ability.

Keywords Tetracycline derivatives · Anti-amyloidogenic activity · Conformational analysis · Continuum solvation models · Geometrical pharmacophore

Electronic Supplementary Material is available for this article if you access the article at http://dx.doi.org/10.1007/s00894-004-0213-x. A link in the frame on the left on that page takes you directly to the supplementary material.

U. Cosentino · M. R. Varí · A. A. G. Saracino · D. Pitea
Dipartimento Scienze dell'Ambiente e del Territorio,
Universitá degli Sudi di Milano-Bicocca,
Piazza della Scienza 1, 20126 Milan, Italy

M. Salmona
Dipartimento Biochimica e Farmacologia Molecolare,
Istituto Mario Negri, Via Eritrea 62, 20157 Milan, Italy

G. Moro (✉)
Dipartimento Biotecnologie e Bioscienze,
Universitá degli Sudi di Milano-Bicocca,
Piazza della Scienza 2, Milan, Italy
E-mail: giorgio.moro@unimib.it
Tel.: +39-02-64483471
Fax: +39-02-64483565

Introduction

Prion diseases are transmissible neurodegenerative disorders that share a similar pathogenic mechanism: the prion protein (PrP) undergoes post-translational modification from a normal cellular isoform (PrP^{C}) to a specific-disease related species (PrP^{Sc}) [1–3]. Circular dichroism (CD) and Fourier-transform infra-red (FTIR) spectroscopy studies indicate that PrP^{Sc} is predominantly β-sheet with a lower proportional α-helical content [4, 5] with respect to PrP^{C}. Moreover, the transition of PrP^{C}–PrP^{Sc} is associated with the acquisition of abnormal chemical-physical properties, including insolubility in non-denaturing detergents, partial resistance to protease digestion and a high tendency to form aggregates and amyloid fibrils [1, 3, 6–8]. According to this view, PrP^{Sc} is responsible for the transmissibility and progression of prion diseases as well as for the brain damage, thus making it a primary target for therapeutic strategies. The need to develop therapies for prion diseases has increased notably since the new variant of Creutzfeldt-Jakob disease (vCJD) emerged, a variant that appears linked causally to bovine spongiform encephalopathy (BSE) [9–11].

Despite the large number of studies on this subject, the molecular mechanism of conversion from PrP^{C} to PrP^{Sc} still remains largely unknown. On the basis of the present knowledge on prion disease, potential therapeutic strategies are: to prevent the formation or induce the degradation of amyloid aggregates; to hinder the conversion process or bind to PrP^{Sc}; to destabilize the PrP^{Sc} structure or interfere with the cellular uptake of PrP^{C}/PrP^{Sc}.

Testing has been carried out on a wide variety of compounds for the treatment of prion diseases [12]. However, the therapeutic use of these compounds is restricted by their intrinsic cytotoxicity and pharmacokinetic properties, as well as by their limited ability to pass the blood/brain barrier. Recently, the anti-prion and the anti-amyloidogenic ability of the TC (TC, compound **1** in Scheme 1) antibiotics were shown by studies performed in vitro [13] and in vivo [12].

The TCs are a group of structurally-related antibiotics used to treat bacterial infections since the 1940s [14]; in the last years they have also achieved importance as inducers of the Tet-Repressor protein [15]. They have very similar chemical structures, derived from a common hydronaphthacene moiety containing four fused rings [16, 17]. The main features required for antibacterial activity are well established [14] and, according to these requirements, the clinically used TCs present various substitutions at the 5, 6 and 7 positions (Scheme 1). These molecules have well characterized pharmacological and pharmacokinetic properties, relatively low toxicity, and some of them are efficient in crossing the blood/brain barrier if an appropriate treatment route is used [18].

The chemistry of TCs in solution is quite complicated due to their ability to adopt different conformations, protonation states, and tautomeric forms, depending on the conditions. Several experimental studies based on CD [19–25] and NMR [26, 27] spectra in solution, and on X-ray crystallographic structure, [28, 29] have shown that TC and its derivatives present different conformations, depending on the pH, the presence of metal cations, and the solvent. The presence of several functional groups with acid-base properties confers an amphoteric character to the TCs [30–33]. The fully protonated form has four dissociable proton centers, namely the C_1–C_3 tricarbonyl methane, the two C_{10}–C_{12} keto-phenolic hydroxyl groups, and the C_4 dimethylammonium group (Scheme 1). On the basis of the generally accepted attribution of the pK_a values to specific functional groups, [33] TC in aqueous solution at neutral pH presents two different forms (Fig. 1): the zwitterionic (ZW) form, in which the hydroxyl group at C_3 is deprotonated while the adjacent 4-NMe_2 group is protonated, and the anionic (ZA) form, in which also the 12-OH group is

Scheme 1 Investigated tetracycline derivatives (see Table 1).

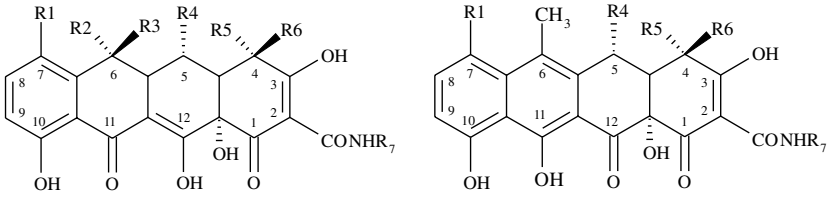

Table 1 Investigated TC derivatives (see Scheme 1)

Id.	Compound	Structure	R_1	R_2	R_3	R_4	R_5	R_6	R_7
1	Tetracycline	I	H	CH_3	OH	H	$N(CH_3)_2$	H	H
2	Anhydrochlortetracycline	II	Cl	–	–	H	$N(CH_3)_2$	H	H
3	Anhydrotetracycline	II	H	–	–	H	$N(CH_3)_2$	H	H
4	Chlortetracycline	I	Cl	CH_3	OH	H	$N(CH_3)_2$	H	H
5	Demeclocycline	I	Cl	H	OH	H	$N(CH_3)_2$	H	H
6	Doxycycline	I	H	CH_3	H	OH	$N(CH_3)_2$	H	H
7	4-Epianhydrotetracycline	II	H	–	–	H	H	$N(CH_3)_2$	H
8	4-Epichlortetracycline	I	Cl	CH_3	OH	H	H	$N(CH_3)_2$	H
9	4-Epioxytetracycline	I	H	CH_3	OH	OH	H	$N(CH_3)_2$	H
10	4-Epitetracycline	I	H	CH_3	OH	H	H	$N(CH_3)_2$	H
11	Meclocycline	I	Cl	$=CH_2$	–	OH	$N(CH_3)_2$	H	H
12	Methacycline	I	H	$=CH_2$	–	OH	$N(CH_3)_2$	H	H
13	Minocycline	I	$N(CH_3)_2$	H	H	H	$N(CH_3)_2$	H	H
14	Oxytetracycline	I	H	CH_3	OH	OH	$N(CH_3)_2$	H	H
15	Rolitetracycline	I	H	CH_3	OH	H	$N(CH_3)_2$	H	$(R_7)^a$

[a] R_7 : $CH_2-N-(CH_2)_3-CH_2$

deprotonated. Moreover, for each protonation state, different tautomers are possible and the tautomeric equilibrium is affected by changes in the environmental conditions [34]. Finally, TC and its analogues undergo complex formation with a variety of the metal cations present in biological fluids, such as Ca(II), Mg(II), Cu(II), Co(II) and Ni(II), [19–22] and this affects chemical as well as conformational equilibria in solutions. Metal-ion coordination is also relevant in determining the biological actions of TC derivatives [16, 19–22]. For instance, it has been shown that the TC interaction with the Tet-repressor receptor involves a TC:Mg^{2+} complex [35].

The anti-prion ability of the TC was shown by in in vitro models [13] by studying the interaction of TC with the PrP aggregates generated by synthetic peptides, homologues to the sequences spanning residues 82–146 (PrP82-146) and 106–126 (PrP106-126) of human PrP; the prevention of PrP peptide aggregation; the reduction of the protease resistance and the disruption of PrP peptide aggregates; and the abolition of neurotoxicity and astroglial proliferation induced by PrP peptides. In an in vivo study [12], TC (**1**) and doxycycline (**6**) significantly delayed the onset of clinical signs of disease and prolonged survival into Syrian hamsters infected with scrapie-infected brain homogenates. Moreover, the reduction of resistance to proteinase K digestion of aggregates of synthetic PrP106–126 peptides (Fig. 2) has recently been measured [12] for the TCs **1**–**15** reported in Scheme 1. Thus, TCs can be considered as candidates for the therapy of prion diseases.

At present, the anti-fibrillogenic mechanism of action of TC derivatives is unknown and the influence on their activity of pH conditions and metal ions has still not been investigated systematically. In particular, although binding of copper and zinc to PrP106–126 has been proposed to modulate the aggregation and neurotoxic properties of this peptide [36], no evidence are present in the literature about the role of cations in the anti-amyloidogenic action of TC derivatives.

A better understanding of the stereoelectronic features of TCs involved in their anti-prion activity could aid to characterize their action mechanism and lead to the design and synthesis of new analogues with better anti-amyloidogenic, pharmacological and financial profiles. Development of TC analogues with strengthened anti-prion activity and devoid of antibiotic effects represents the general aim of our research.

As a first step, we present here an investigation of the conformational behavior in aqueous solution of the 15 TCs of Scheme 1 in the ZW and ZA forms, with the aim of searching for the presence of a geometrical pharmacophore able to explain the ability to reduce the proteinase K resistance of PrP 106–126 aggregates.

Theoretical investigations by means of molecular mechanics (MM) as well as quantum-mechanical semiempirical and ab initio methods have been carried out to assess the conformational behavior of the different forms of TCs both in vacuo [37] and in aqueous solution [38–42]. Recently, the conformations and the tautomeric forms of neutral TC have been investigated [38] at the B3LYP/6-31G* and MP2/6-31G* levels in aqueous solution by the polarizable continuum model (PCM) [43–45]. Different tautomers were considered: the non ZW form, the ''conventional'' zwitterion, and other ''non-conventional'' zwitterions. Six different tautomeric forms were found to lie within 10 kcal mol^{-1} of the most stable one, showing two main conformations: an *extended* and a *folded* one (labeled as conformation 1 and 2 in reference [38]). Moreover, for each tautomer the *extended* conformation was more stable than the *folded* one.

These findings suggest that the results of our present investigation, focused on the search for a geometrical pharmacophore, should not be affected by the presence

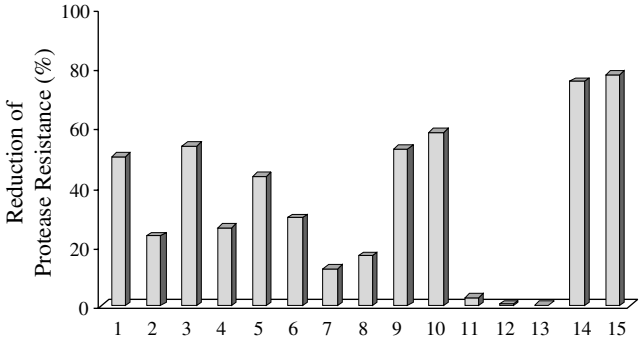

Fig. 2 Reduction of resistance to protease K digestion of PrP 106-126 aggregates incubated with the **1**–**15** TC derivatives [12]

Fig. 1 Schematic representation of the structure of TC in the ZW and ZA forms and atom numbering

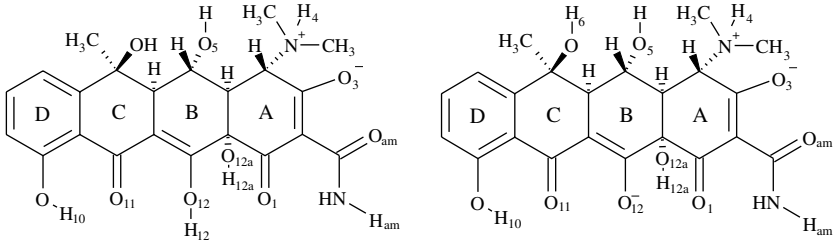

of different tautomers for each protonated state; therefore, only the tautomers highlighted in Fig. 1 will be considered from hereon in for the ZW and ZA forms.

Although the combination of MM methods with continuum solvation models is one of the most common methods of establishing the possible conformations of molecules in solution, important problems are still present, mainly arising from the quality of the parameter set. Thus, to test the reliability of the MM method on this class of compounds, we will compare the MM results on TC with those obtained at ab initio level.

Material and methods

The X-ray structure taken from the Cambridge crystallographic database [46] (CCD reference code tetcyh10 [28]) was used as the input geometry for TC. The conformational search was carried out on the ZW and ZA forms. The MacroModel 7.2 [47] implementations of the original MM2 [48] and Amber [49] force fields were used in combination with the generalized Born-solvent accessible surface area (GB-SA) continuum solvation model [50, 51]. The conformational space of the ZW and ZA forms of TC was investigated by the Monte Carlo multiple minimum (MCMM) procedure (5,000 steps). [52, 53]. Ten inter-ring torsional angles of the hydronaphthacene moiety were rotated from 0° to 180° with random variations. Full energy minimization was performed for each generated conformation, discarding conformations 25 kcal mol^{-1} above the global minimum. Redundant conformations were removed on the basis of the root mean square (RMS) values between the hydronaphthacene carbon atoms, because our main interest was focused on the flexibility of the ring system. Finally, stationary points were characterized as minimum energy conformations by frequency analysis. To search for geometrical similarity among the different conformers, the minima obtained were submitted to a hierarchical cluster analysis (complete linkage method, STATISTICA software package [54]) using the values of the ten inter-ring torsional angles. The MM2 lowest energy conformation in each cluster was fully optimized at the RHF/6-31G** level with the Gaussian98 program [55], using the conductor like-polarixable continuum modes (C-PCM) [43, 44], and the united atom topological model [56] to generate the solute cavity. Single point energy calculations were performed on the optimized structures[1] at the DFT level, using the PBE0 functional [58], and the 6-31 + G** basis sets.

[1]Due to slow convergence the optimization was, in some cases, stopped whether convergence parameters were less than twice the default values. For this reason, frequency analysis was not performed, and the final geometries correspond to stable conformations for the chosen minimization algorithm, rather than true minima.

On the basis of the results obtained on TC, the MCMM conformational search of the derivatives **2**–**15** in the ZW and ZA forms was carried out using the MM2/GB-SA method, using the computational protocol described previously.

Results and discussion

The MM2 conformational analysis in aqueous solution of compound **1** provided 19 unique minimum-energy conformations for both the ZW and the ZA forms (Table S1 in the Supplementary Material). The Amber force field generated many more minimum-energy conformations than MM2: 30 and 33 conformers for the ZW and ZA forms, respectively.

The conformational search generated a set of conformers with great geometrical flexibility of the hydronaphthacene moiety. In general, the main conformational variability is observed in the A and B rings, as the A–B connection is more flexible than the B–C one. Results of the cluster analysis, performed on both MM2 and Amber minimum-energy conformations, are reported as dendograms in Figs. 3 and 4 for the ZW and the ZA forms, respectively.

Each of the six clusters identified, labeled from **a** to **f**, contains both MM2 and Amber conformations, highlighting that both force fields find similar minimum energy conformations. Superimposition of the molecular structures showed that the geometries within each cluster were not significantly different, but that the geometries of the different clusters themselves were dissimilar.

Dendogram analysis shows two main different conformational arrangements of the hydronaphthacene moiety named, in accordance with the literature, [19] the *extended*-like conformation (clusters **a**, **b**, and **e**) and the *folded*-like conformation (clusters **c**, **d**, and **f**). The molecular structure of the lowest-energy conformation in each cluster is reported in Fig. 5.

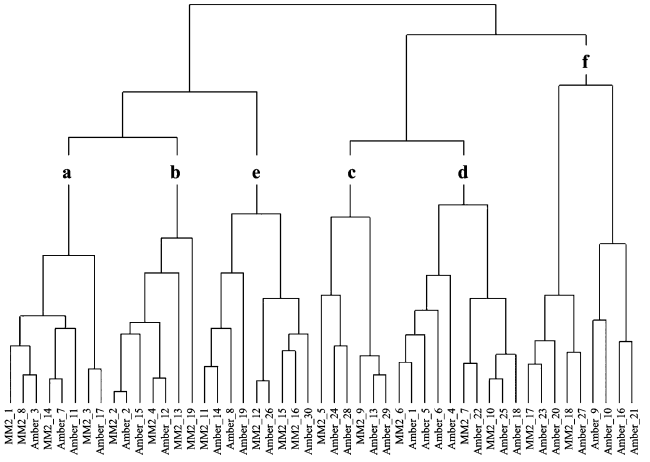

Fig. 3 Dendogram of the MM2 and Amber minimum energy conformations of the ZW form of compound **1**

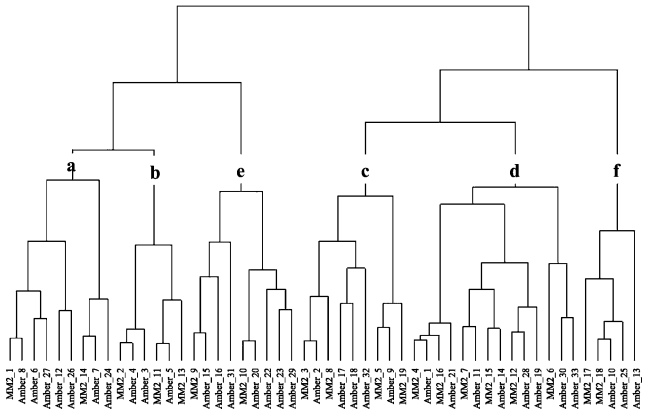

Fig. 4 Dendogram of the MM2 and Amber minimum energy conformations of the ZA form of compound **1**

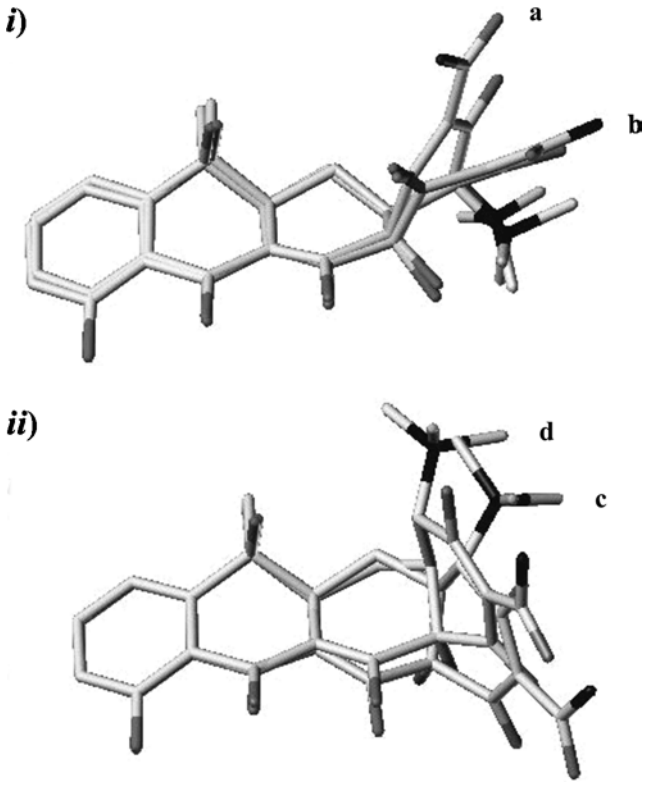

Fig. 5 Molecular structures of the lowest energy conformations present: (1) in clusters **a** and **b** (*extended* conformations); (2) in clusters **c** and **d** (*folded* conformations). Hydrogen atoms not reported, with the exception of the 4-HN(Me)$_2$ one

In the *extended* conformations, the B, C, and D rings approximately lie on a common plane and the C_1, C_2, C_3 and amide carbons lie above this plane. The *folded* conformations differ from the *extended* ones in that they have a different spatial arrangement of the A-ring: the *folded* conformations are formally derived from the *extended* ones by an interconversion process that involves rotation around the C_{4a}–C_{12a} bond, causing the A-ring to be more folded towards the B-ring.

To compare the conformational behavior of TC in different protonation states, we took together all MM2 conformers of ZW and ZA forms and submitted the new set to cluster analysis. Results show (Fig. 6) that conformations of both forms are present in each cluster, and generally with the same original cluster label. Thus, it can be concluded that in the two different protonated states, the four-ring system has similar minima and similar conformational flexibility; the same result was found previously for neutral TC considering different tautomeric forms [38].

A possible key to achieve maximum reading comprehension of the observed conformational flexibility could be the formation of different hydrogen bond networks in TC. For this reason, the hydrogen-bond pattern of the MM2 conformers was analyzed for each form (Table S2 in the Supplementary Material). Independently of the protonation state, conformations belonging to the same cluster show similar hydrogen-bond networks. Only conformations in cluster **a** show a hydrogen bond between the two cis substituents of the A ring, the hydrogen of the protonated amine at C_4 and the oxygen at the C_{12a} center. This interaction seems to be the most important factor in determining the *extended* conformation adopted by the hydronaphthacene moiety in this cluster. Although this interaction is not present in cluster **b**, the H-bond networks in clusters **a** and **b** are similar. Thus, the H-bond between the oxygen at C_{12} and the hydroxyl hydrogen at C_{12a} is present only in these two clusters. As a result, the conformations in cluster **b** resemble those in cluster **a** but show a less extended arrangement of the four-ring system, named *twisted* in accordance with the literature [19]. The conformational characteristics of clusters **c**–**e** are determined by other hydrogen bond patterns, such as the $O_1 \cdots H_{12a}$ hydrogen bond present only in these clusters.

The results of our conformational analysis are in agreement with available experimental data. The interpretation of CD spectra [19–22, 25] has shown that, in

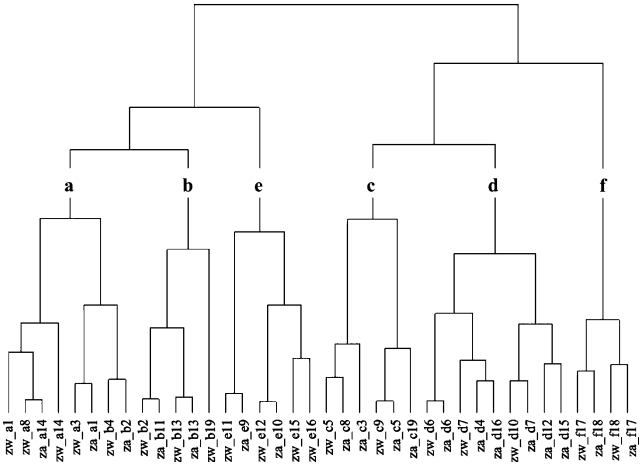

Fig. 6 Dendogram of the MM2 minimum energy conformations of the ZW and ZA forms of compound **1**

aqueous solution, TC presents two conformations, one *extended* the other *twisted* depending on the pH. The *twisted* conformation is found in the crystallographic structure of the TC hydrated crystal [28], while the *folded* conformation is observed for the anhydrous crystals of compound **14**, the oxytetracycline [28, 29]. The good superimposition of the hydronaphthacene moiety between the crystal structures and the lowest energy conformations of clusters **b** and **d** (RMS = 0.148, 0.304 Å respectively) supports the reliability of our results.

Tables 2 and 3 report the conformational energies in each cluster for the ZA and ZW forms, respectively. By considering the lowest energy conformation within each cluster, it is evident that the two force fields provide different energetic scales. For both forms, the MM2 sequence is: *extended* conformation **a**, *twisted* conformation **b** and *folded* conformation **d**. On the contrary, Amber identifies the *folded* conformation **d** as the global minimum, with the **a** and **b** conformations being at highest energy.

Given the observed discrepancy in the conformational energies of the two force fields, we tested the reliability of the MM results by ab initio calculations. The geometry of the MM2 conformations with the lowest relative energy within each cluster for both the ZW and the ZA forms of TC were fully optimized by means of ab initio methods, including solvent effects by the PCM approach. The RMS values calculated for the superimposition of the hydronaphthacene moiety between the structures of both force fields and the ab initio structures are reported in Tables 4 and 5, together with the relative conformational energies. In general, for ZW the MM2 geometries compare well with the corresponding ab initio structures, but there was poorer agreement for ZA. As previously observed, the two force fields give similar geometries, thus we can conclude that the Amber geometries are also satisfactory.

As far as concerns the conformational energies, the ab initio results show (Tables 4, 5) the *twisted* **b** conformation as the most stable in both the ZW and ZA forms, while the *extended* **a** conformation and the *folded*

Table 2 Relative energies, ΔE (kcal mol^{-1}), of conformers within 10 kcal mol^{-1} above the global minimum, for the ZW species of compound **1** calculated in aqueous solution by the MM2 and the Amber force fields

Cluster	Id	ΔE (MM2)	Id	ΔE (Amber)
a	**1**	**0**	*3*	2.13
	3	2.35	7	4.94
	8	6.07	11	6.44
b	**2**	**1.98**	2	1.39
	4	3.98	12	6.55
	13	9.56	15	7.89
c	**5**	**4.15**	13	6.55
	9	6.26		
d	**6**	**5.04**	1	0
	7	5.14	4	2.87
	10	6.64	5	2.93
			6	3.67
			18	9.52
e	**11**[a]	**6.78**	8	5.10
	12	**8.47**	14	7.74

In bold, the MM2 conformations chosen for ab initio geometry optimization

[a]ab initio optimization of this structure did not converged

Table 3 Relative energies, ΔE (kcal mol^{-1}), of conformers within 10 kcal mol^{-1} above the global minimum, for the ZA species of compound **1** calculated in aqueous solution by the MM2 and the Amber force fields

Cluster	Id	ΔE MM2	Id	ΔE Amber
a	**1**	**0**	6	4.10
			7	4.48
			8	4.54
			12	7.71
b	**2**	**0.34**	3	0.56
	11	8.32	4	1.18
	13	9.5	5	1.21
c	**3**	**2.91**	2	0.45
	5	3.88	9	4.68
	8	6.77		
d	**4**	**3.56**	1	0
	6	5.75	11	6.63
	7	5.87		
	12	9.19		
e	**9**	**7.98**		
	10	8.17		

In bold, the MM2 conformations chosen for ab initio geometry optimization

Table 4 Relative energies, ΔE (kcal mol^{-1}), of conformers for the ZW form of compound **1** calculated in aqueous solution by the MM (MM2 and Amber) and the ab initio methods, and RMS values (Å) (see text)

Cluster	PBE0/6-31+G**		MM2			Amber		
	Id	ΔE	Id	RMS	ΔE	Id	RMS	ΔE
a	1	2.19	1	0.178	0	3	0.158	2.13
b	2	0	2	0.062	1.98	2	0.114	1.39
c	5	3.83	5	0.192	4.15	6	0.201	3.67
d	6	5.44	6	0.118	5.04	1	0.178	0
e	12	10.42	12	0.083	8.47	8	1.019	5.10

Table 5 Relative energies, ΔE (kcal mol^{-1}), of conformers for the ZA form of compound **1** calculated in aqueous solution by the MM (MM2 and Amber) and the ab initio methods, and RMS values (Å) (see text)

Cluster	PBE0/6-31+G**		MM2			Amber		
	Id	ΔE	Id	RMS	ΔE	Id	RMS	ΔE
a	1	1.57	1	0.434	0	8	0.540	4.54
b	2	0	2	0.405	0.34	3	0.490	0.56
c	3	5.30	3	0.148	2.91	2	0.211	0.45
d	4	5.90	4	0.482	3.56	1	0.305	0
e	9	7.42	9	0.169	7.98	15	0.230	11.16

Table 6 Conformations of compounds **1**–**15** in the ZW form present in cluster **a**–**e**. Cluster labels are those of the TC conformations present in the clusters (see Table 2)

Cluster labels	a/e	b/a	c/e	d/c	d
1	1, 8, 11	2, 3, 4, 13	9, 12	5, 6, 7	10
2	5	1		2	3, 4
3		2, 1		3	4, 5
4	1, 12, 13, 15, 16, 17	2, 3, 4, 5, 7	6, 10	8, 9, 11, 14	
5	1, 6, 7	2, 4, 9		3, 5, 8	
6	1, 15, 16, 17, 19, 20, 21	2, 3, 4, 6, 18, 22	9, 13	5, 7, 8, 10	11, 12, 14
7		1			
8	1, 2, 4, 6	3, 5, 7, 9	8, 10		11
9	1, 2, 7	3, 4, 5, 6, 8, 11, 12	9	10	13
10	1, 2, 4	3, 5			
11	1, 3, 13, 14, 11	2, 7, 10, 15	5, 9, 12	4, 6, 8	
12	1, 3, 11, 15, 16, 13	2, 10, 6, 12	4, 9, 14	5, 7, 8	
13	1, 5, 6	2	8	3, 4	7
14	1, 19, 20, 14, 16, 18	2, 3, 4, 7, 8, 9, 17	10, 12, 13	5, 6, 15	11, 21
15	8, 16, 12, 13, 14	1, 2, 3	9, 15	4, 5, 6, 7	10, 11

Table 7 Conformations of compounds **1**–**15** in the ZA form present in cluster **a**–**e**. Cluster labels are those of the TC conformations present in the clusters (see Table 3)

Cluster labels	a	b	c	d	e
1	1	2, 11, 13	3, 5, 8	4, 6, 7, 12	9, 10
2		2, 4		1, 3	
3		2, 4		1, 3, 5	
4	3	1, 2, 6, 7, 14	4, 8	5, 10, 11, 12, 15	9, 13
5	5, 1	3, 2, 8, 13	6, 7, 12	4, 9, 11	10
6	1, 8	2, 6	4, 5, 7, 13	3, 9, 10, 11	12
7		1, 2		3, 4	
8		1, 2			
9	2, 7, 5	1, 3, 4, 6, 8, 9	11, 12		10
10	2, 4	1, 3			
11	7	1, 2, 5, 11, 12	4, 6	3, 8, 9, 14	10, 13
12	2, 10, 9	1, 5, 15, 16	4, 6, 13	3, 7, 8, 12, 14	11, 17
13	2	1, 4, 6, 11	5, 8	3, 7, 9	10
14	3, 9	1, 2, 5, 6	4, 7, 10	8, 11, 13	12
15	12, 13, 15	1, 2, 6, 11, 14	3, 5, 8	4, 7, 9, 10, 16	17

d conformation are 1.5–2.2 and 5.5–6.0 kcal mol^{-1} above the global minimum, respectively. The stability sequence obtained compares well with that reported for neutral TC [38].

In general, MM2 conformational energies show a better agreement with those calculated ab initio, while Amber identifies the *folded* **d** conformation as the global minimum.[2]

Thus, for TC we can conclude that both force fields provide reliable geometries, but the MM2 conformational energies are more reliable than the Amber ones. For this reason the conformational analysis of the TC derivatives **2**–**15** was carried out using the MM2 force fields for the ZW and ZA forms.

In general, all the TC derivatives present both *extended*- and *folded*-type conformations, as already found for TC, with a large number of conformations within 10 kcal mol^{-1} above the global minimum, reflecting the conformational flexibility of the hydronaphthacene moiety (Tables S3 and S4 in the Supplementary Material). The anhydrous analogues **2**, **3**, and **7** show fewer conformations than the other derivatives because of the aromatic character of the C ring, which reduces the flexibility at the B–C ring junction.

With the aim of searching for a geometrical pharmacophore, a hierarchical cluster analysis was performed on the conformations of compounds **1**–**15**, for both the ZW and ZA forms. The resulting dendograms (Figs. S1, S2 in Supplementary Materials) show a clear separation of the *extended* and the *folded* conformer families, and the conformations of all compounds are grouped in the same five clusters (**a**–**e**) found for TC (Tables 6 and 7).

The TC derivatives in the ZW form present an *extended* conformation, analogous to the TC conformation of cluster **a**, as global minimum. The exceptions are the most active compound **15** and the less active, or inactive, anhydrous analogues **2**, **3**, and **7** where the global minimum is a *twisted* conformation that resembles the TC conformation of cluster **b**. In contrast, the global minima of the ZA form adopt the TC *twisted* conformation

[2]The RMS values between molecular mechanics and the ab initio relative energies highlight the agreement between MM2 and the *ab initio* results, and the less satisfactory performance of Amber: for MM2 and Amber the RMS values for ZW are 1.59 and 3.46 kcal mol^{-1} respectively, and for ZA 1.68 and 4.07 kcal mol^{-1}.

of cluster **b**, with the exception of compounds **2**, **3** and compounds **5**, **6** that adopt a *folded* **d** and an *extended* **a** conformation respectively.

For both forms, cluster **b** always presents at least one conformation of each compound, and thus cannot discriminate between compounds with different biological activity. On the other hand, there are no clusters containing only conformations of active compounds, nor was there a cluster containing only conformations of poorly active or inactive compounds.

Thus the present results do not support the presence of a geometrical pharmacophore and, despite the wide conformational flexibility showed by the TC derivatives, it seems that other properties play a crucial role in determining their anti-fibrillogenic ability.

Conclusions

The MCMM protocol, in conjunction with MM force fields, provides an exhaustive sampling of the potential energy surface of TCs, and is able to generate different conformational families. Comparison with ab initio results shows that the conformational behavior of this class of compounds is reasonably well predicted by the general-purpose MM2 force fields, while the Amber force fields provide unreliable conformational energies.

Overall, the present conformational study on the TC derivatives considered has highlighted a quite relevant conformational flexibility in aqueous solution of the hydronaphthacene moiety. Nevertheless, all compounds showed very similar accessible conformations and the ZW and ZA forms present similar conformational behavior. As a consequence, the conformational flexibility of the TC derivatives is of no relevance whatsoever to the observed activity, and no geometrical pharmacophore can be defined.

Other stereo-electronic properties, influenced by protonation state, tautomeric equilibria and metal ion complexation, should play a crucial role in determining the anti-fibrillogenic ability of TC derivatives. The next step of our research will thus concern the comparison of stereo-electronic properties of TC derivatives within the framework of a three dimensional quantitative structure activity relationships (3D-QSAR) approach.

Unveiling of the relationship existing between molecular properties of TCs and their anti-fibrillogenic activity will enable us to develop more effective analogues capable to cross the blood/brain barrier and devoid of antibacterial activity.

Supplementary Material available

SuppMat-Figs.doc Dendograms from hierarchical cluster analysis of the MM2 conformations of the ZW (Fig. S1) and the ZA (Fig. S2) forms of compounds **1**–**15**.

SuppMat-Tabs.doc Total number and energy range distribution of conformations of the ZW and ZA forms of compound **1** (Table S1) and of the ZW (Table S3) and ZA (Table S4) forms of compounds **1**–**15**; hydrogen bond pattern of MM2 conformers for the ZW and ZA forms of compound **1** (Table S2).

Acknowledgements We gratefully acknowledge financial support from the Italian Ministry of University and Research (PRIN 2001 and PRIN 2003).

References

1. Prusiner SB (1991) Science 252:1515–1522
2. Prusiner SB (1997) Science 278:245–251
3. Prusiner SB, Scott MR, De Armond SJ, Cohen FE (1998) Cell 93:337–348
4. Caughey BW, Dong A, Bhat KS, Ernst D, Hayes SF, Caughey WS (1991) Biochemistry 30:7672–7680
5. Pan KM, Baldwin M, Nguyen J, Gasset M, Serban A, Groth D, Mehlhorn I, Huang Z, Fletterick RJ, Cohen FE, Prusiner SB (1993) Proc Natl Acad Sci U S A 90:10962–10966
6. Bolton DC, McKinley MP, Prusiner SB (1982) Science 218:1309–1311
7. McKinley MP, Bolton DC, Prusiner SB (1983) Cell 35:57–62
8. De Armond SJ, McKinley MP, Barry RA, Braunfeld MB, McColloch JR, Prusiner SB (1985) Cell 41:221–235
9. Will RG, Ironside JW, Zeidler M, Cousens SN, Estibeiro K, Alperovitch A, Poser S, Pocchiari M, Hofman A, Smith PG (1996) Lancet 347:921–925
10. Collinge J, Sidle KCL, Heads J, Ironside J, Hill AF (1996) Nature 383:685–690
11. Bruce ME, Will RG, Ironside JW, McConnell I, Drummond D, Suttle A, McCardle L, Chree A, Hope J, Birkett C, Cousens S, Fraser H, Bostock CJ (1997) Nature 389:498–501
12. Forloni G, Varí MR, Colombo L, Bugiani O, Tagliavini F, Salmona M (2003) Curr Med Chem—Imun, Endoc and Metab Agents 3:185–197
13. Forloni G, Angeretti N, Chiesa R, Monzani E, Salmona M, Bugiani O, Tagliavini F (1993) Nature 362:543–545
14. Chopra I, Roberts M (2001) Microbiol Mol Biol Rev 65:232–260
15. Hillen W, Behrens C (2002) BIOspektrum 8:355–358
16. Mitscher LA (1978) Medicinal Research Series, vol 9. The chemistry of antibiotics. Marcel Dekker, New York
17. de Leenheer AP, Nelis HJCF (1979) J Pharm Sci 68:999–1002
18. Sande MA, Mandell GL (1990) Tetracyclines, chloramphenicol, erythromycin, and miscellaneous antibacterial agents. In: Goodman Gilman A, Rall TW, Nies AS, Taylor P (eds) The pharmacological basis of therapeutics, 8th edn. Pergamon Press, New York, pp 1117–1145
19. Lambs L, Decock-Le Reverend B, Kozlowski H, Berthon G (1988) Inorg Chem 27:3001–3012
20. Lambs L, Berthon G (1988) Inorg Chim Acta 151:33–43
21. Lambs L, Brion M, Berthon G (1985) Inorg Chim Acta 106:151–158
22. Brion M, Lambs L, Berthon G (1986) Inorg Chim Acta 123:61–68
23. Mitscher LA, Bonacci AC, Sokoloski TD (1968) Tetrahedron Lett 51:5361–5364
24. Mitscher LA, Slater-Eng B, Sokoloski TD (1972) Antimicrob Agents Chemother 2:66–72
25. Hughes LJ, Stezowsky JJ, Hughes RE (1979) J Am Chem Soc 101:7655–7657
26. Williamson DE, Everett JrGW (1975) J Am Chem Soc 97:2397–2405
27. Gulbis J, Everett Jr GW (1975) Tetrahedron 32:913–917

28. Stezowski JJ (1976) J Am Chem Soc 98:6012–6018
29. Prewo R, Stezowski JJ (1977) J Am Chem Soc 99:1117–1121
30. Dos Santos HF, De Almeida WB, Zerner MC (1998) J Pharm Sci 87:190–195
31. Duarte HA, Carvalho S, Paniago EB, Simas AM (1999) J Pharm l Sci 88:111–120
32. Stuer-Lauridsen F, Birkved M, Hansen LP, Holten Lützhøft HC, Halling-Sørensen B (2000) Chemosphere 40:783–793
33. Tavares MFM, McGuffin L (1994) J Chrom A 686:129–142
34. Schneider S (2001) Proton and metal ion binding of tetracyclines. In: Greenwald RA, Hillen W, Nelson M (eds) Tetracyclines in biology, hemistry and medicine. Birkhaüser, Basel, pp 65–104
35. Hinrichs W, Kisker C, Duevel M, Mueller A, Tovar K, Hillen W, Saenger W (1994) Science 264:418–420
36. Jobling MF, Huang X, Stewart LR, Barnham KJ, Curtain C, Volitakis I, Perugini M, White AR, Cherny RA, Masters CL, Barrow CJ, Collins SJ, Bush AI, Cappai R (2001) Biochemistry 40:8073–8084
37. Lanig H, Gottschalk M, Schneider S, Clark T (1999) J Mol Model 5:46–62
38. Othersen OG, Beierlein F, Lanig H, Clark T (2003) J Phys Chem B 107:13743–13749
39. Duarte HA, Carvalho S, Paniago EB, Simas AM (1999) J Pharm Sci 88:111–120
40. Dos Santos HF, De Almeida WB, Zerner MC (1998) J Pharm Sci 87:190–195
41. de Almeida WB, Dos Santos HF, Zerner MC (1998) J Pharm Sci 87:1101–1108
42. de Almeida WB, Costa LRA, Dos Santos HF, Zerner MC (1997) J Chem Soc, Perkin Trans 2: Physical Organic Chemistry 1335–1339
43. Amovilli C, Barone V, Cammi R, Cances E, Cossi M, Mennucci B, Pomelli CS, Tomasi J (1998) Adv Quantum Chem 32:227–261
44. Barone V, Cossi M (1998) J Phys Chem A 102:1995–2001
45. Tomasi J, Persico M (1994) Chem Rev 94:2027–2094
46. Bruno IJ, Cole JC, Lommerse JPM, Rowland RS, Taylor R, Verdonk ML (1997) J Comput-Aided Mol Des 11:525–537
47. Mohamadi F, Richards NGJ, Guida WC, Liskamp R, Lipton M, Caufield C, Chang G, Hendrikson T, Still WC (1990) J Comput Chem 11:440–467
48. Allinger NL (1977) J Am Chem Soc 99:8127–8134
49. Weiner SJ, Kollman PA, Case DA, Singh UC, Ghio C, Alagona G, Profeta S, Weiner P (1984) J Am Chem Soc 106:765–784
50. Still WC, Tempczyk A, Hawley RC, Hendrickson T (1990) J Am Chem Soc 112:6127–6129
51. Weiser J, Weiser AA, Shenkin PS, Still WC (1998) J Comput Chem 19:797–808
52. Chang G, Guida WC, Still WC (1989) J Am Chem Soc 111:4379–4386
53. Saunders M, Houk KN, Dong Wu Y, Still CW, Lipton M, Chang G, Guida WC (1990) J Am Chem Soc 112:1419–1427
54. STATISTICA 5.1 for Windows (1998) StatSoft Inc, Tulsa, OK 74104
55. Frisch MJ, Trucks GW, Schlegel HB, Scuseria GE, Robb MA, Cheeseman JR, Zakrzewski VG, Montgomery JA, Stratmann RE Jr, Burant JC, Dapprich S, Millam JM, Daniels AD, Kudin KN, Strain MC, Farkas O, Tomasi J, Barone V, Cossi M, Cammi R, Mennucci B, Pomelli C, Adamo C, Clifford S, Ochterski J, Petersson GA, Ayala PY, Cui Q, Morokuma K, Malick DK, Rabuck AD, Raghavachari K, Foresman JB, Cioslowski J, Ortiz JV, Stefanov BB, Liu G, Liashenko A, Piskorz P, Komaromi I, Gomperts R, Martin RL, Fox DJ, Keith T, Al-Laham MA, Peng CY, Nanayakkara A, Gonzalez C, Challacombe M, Gill PMW, Johnson B, Chen W, Wong MW, Andres JL, Gonzalez C, Head-Gordon M, Replogle ES, Pople JA (1998) Gaussian 98 (Revision A.7). Gaussian Inc, Pittsburgh, PA. Description of the basis sets and explanation of standard levels of theory can be found in [58]
56. Barone V, Cossi M, Tomasi J (1997) J Chem Phys 107:3210–3221
57. Adamo C, Barone V (1999) J Chem Phys 110:6158–6170
58. Foresman JB, Frisch AE (1996) Exploring chemistry with electronic structure methods. Gaussian Inc, Pittsburgh, PA